Activation and control of organolanthanide synthesis by supersonic molecular beams: Erbium-porphyrin test case

Marco Nardi,[1] Roberto Verucchi,[1] Riccardo Tubino,[2] and Salvatore Iannotta[1,3,*]

[1]*Istituto di Fotonica e Nanotecnologie (IFN), Consiglio Nazionale delle Ricerche (CNR), Via alla Cascata, 56/C-Povo, 38100 Trento, Italy*

[2]*Dipartimento di Scienza dei Materiali, Università di Milano Bicocca, Via R. Cozzi, 53-20125 Milano, Italy*

[3]*Istituto dei Materiali per l'Elettronica ed il Magnetismo (IMEM), CNR, Parco Area delle Scienze, 37/a, 43100 Parma, Italy*

(Received 17 June 2008; revised manuscript received 12 November 2008; published 4 March 2009)

Hybrid Er-Tetraphenylporphyrin (Er-TPP) thin films have been synthesized on a SiO_2/Si(100) substrate in a co-deposition approach that combines an H_2TPP seeded supersonic molecular beam and an effusive molecular beam of the metal. As confirmed by detailed surface electron spectroscopies, our experiments in ultrahigh vacuum demonstrate the ability to produce and control the chemical reactivity between the two species on the surface of the growing film. This is achieved by fully exploiting the unique features of the supersonic molecular-beam deposition approach in a co-deposition scheme that we show to be ideally suited to induce and control chemical reactivity. We believe that the ability to synthesize organolanthanides films, showing a thickness that is suitable for applications in optoelectronics, could pave the way to a class of devices based on active materials chemically engineered via this solid-state/vapor phase approach in vacuum.

DOI: 10.1103/PhysRevB.79.125404 PACS number(s): 81.10.Bk, 82.30.−b, 81.15.Hi

I. INTRODUCTION

Among π-conjugated organic molecules, porphyrins are attractive for their optical properties, in terms of a wide absorption band and efficient photoluminescence. On the other hand, lanthanides and in particular erbium are widely used as photoluminescent materials in photonic and optoelectronic devices for telecommunications. The combination of these features, achievable in an organolanthanide hybrid complexes, is hence highly promising for a class of devices where the organic part would play the role of an antenna, that is, it captures energy from light absorption (or by electrical stimulation) and transfers it to the metal counterpart, which in turn gets excited and then decays by luminescence.[1–6]

The growing interest in organic molecules as active elements for devices is mainly driven by the ability of tuning their chemical reactivity, electronic, and optical properties by chemical design and engineering.[7] They are particularly promising for application in photonics and optoelectronics, where the ability to tune the optical response and efficiency has opened new perspectives.[8] The aim of realizing extensive optoelectronic applications still faces some difficulties, mainly related to the control of properties at the interfaces and to the limited carrier mobilities achievable. Strategies to overcome such shortcomings, together with the synthesis of novel molecules, include improvement in controlling film structure and morphology during growth.[9]

Among organic molecules, a leading role is played by large macrocycles, e.g., porphyrins, suitable in several technological applications for their intense optical absorption and photoluminescence yield. Porphyrins are involved in key processes such as the synthesis of the heme group (the portion of hemoglobin devoted to transport and delivering of oxygen in the human body) and phototherapy by the oxygen singlet generation.[10] They also play an important enzymatic action (VitB12) and act as intense colorant (chlorophyll). Porphyrins are hence extensively used in organic or hybrid photovoltaic cells research, or as active element for sensing or catalysis.[11] Lanthanides complexes are attracting increasing interest as visible emitters due to their enhanced efficiency and color purity. In these complexes, the excited-state levels of the emitting ion are not directly pumped but are populated by an efficient intramolecular energy transfer from the optically (possibly electrically) excited ligands, which act as efficient light harvesting antenna. This approach allows the specific optimization of each moiety for the particular function (absorption, transport, emission) to which it is dedicated.[1–6]

Elements of the lanthanides series are well-known emitters in the visible and infrared regions.[12,13] The triply-charged ions are characterized by $4f$ states with atomiclike properties that, in presence of a weak field, show several radiative or nonradiative de-excitation pathways. For instance, erbium emits at about 700, 980, and 1500 nm, the latter being a band strategic for telecommunications. The dispersing Er^{3+} ions in solid-state matrixes, silica in particular, has given rise to a very active material research field, producing technologically relevant applications.[14] One of the major aims at present is to find ways to overcome the limitations in luminescence yields arising from both the relatively low erbium concentrations achievable ($1\times10^{19}-1\times10^{20}$ atoms/cm^3), due to the onset of processes of coalescence, and the quenching of the radiation, due to the presence of water (O-H group) and of C-H bonds. These groups drastically decrease the lifetimes of the excited state of erbium ions, strongly quenching the infrared emission.[12,13] Another shortcoming arises from the laser radiation needed to excite the lanthanide ion, a technology somewhat expensive and cumbersome that consequently limits the use of lanthanides in telecommunications.

Organolanthanides hybrids are typically synthesized by wet chemistry starting from specific precursors in solution.[15] It is a well-established and reliable approach, yielding the correct ionic state of the lanthanide in the organic molecule,

with the desired chemical coordination. These are crucial points to achieve efficient energy transfer between the ligand and the metal. Films are then typically obtained by spin coating from a solution or by sol-gel methods.[6,16] Such an approach is not best suited for vacuum-based technologies of microelectronics. That is why vacuum sublimation of previously synthesized organic-inorganic materials is widely explored, sometimes including detailed surface electronic characterizations. In fact metal phthalocyanines,[17–19] including Er-phthalocyanines,[20] have been the subject of several studies, while only a few works deal with free base porphyrins,[21,22] as well as metal porphyrins,[23–27] and there are no reports on erbium porphyrins.

A strategy toward better performing devices could strongly benefit from an alternative approach where the synthesis and the growth of the films are improved, in particular extending the control on the stoichiometry and structure or morphology of the material. In vacuum synthesis of hybrid materials has been very recently explored by "metalation" experiments of a monolayer of porphyrin molecules deposited on ordered Ag or Au surfaces, using molecular beams of the pure organic and inorganic counterparts.[28–30] There the formation of the host-guest complex is achieved by a multistep chemical process that requires moderate substrate temperatures (550 K), as it is the case for Zn.[29] Only for Co, the reaction occurs at room temperature likely with a significant contribution from intense charge-transfer processes between the host metal atom and the Ag surface.[28,30] We have developed an approach that combines co-deposition from porphyrin supersonic molecular beams and atomic Er beams. This approach to the synthesis of hybrid complexes is particularly interesting since the physical and chemical reactions leading to the formation of hybrids could be controlled and studied in details *in situ*, aiming at understanding the role of the state of the precursor and of the substrate surface and hence revealing chemical pathways and processes possibly different from those observed in liquid reactions. The supersonic molecular-beam deposition (SuMBD) approach that we adopt here has already demonstrated the ability to control physical/chemical processes occurring during thin-film growth of both organic and inorganic materials.[9,31–40] A supersonic molecular beam of organic molecule is generated from a gas mixture of a carrier gas (usually a noble gas), seeded by the molecules of the specific substances and experiencing a supersonic expansion in vacuum. The generated hyperthermal beam has properties that are very different from an effusive molecular beam[31,32] (Knudsen cell). Heavier species in the beam undergo an aerodynamic acceleration that, depending on the mass ratio between gas carrier and organic molecule, leads to kinetic energies (KEs) as high as several tens of eV, with a substantial freezing of rotations and low-lying energy vibrations. The beam has a high spatial anisotropy, with a flux extremely focused in the forward direction, leading to a divergence of only a few degrees or less. The final physical state of particles is tunable by acting on the operating parameters of the beam source, the latter being an oven having a micrometric aperture (nozzle). In particular, since the sublimation temperature and the carrier gas pressure strongly influence the particles dilution in the beam, they are the simplest parameters to play with to control the final kinetic energy of the molecules seeding the beam.

The SuMBD approach has been successfully used in our laboratory to synthesize microcrystalline cubic β-SiC on the Si(111)7×7 surface via fullerene supersonic beams.[33,34] In this way, we lowered significantly the temperature of the carbide synthesis, with respect to molecular-beam epitaxy (MBE). We ascribed this effect to the kinetically activated reactivity at the Si surface of the C_{60} precursor when its KE becomes large enough (>25 eV). The material structure was cubic SiC(3C) and it has been obtained without any need of post deposition thermal treatments (as typical of other approaches), indicating that the process activated by the fullerene high KE can also induce structural ordering. Thin films of organic molecules deposited by SuMBD have shown structural properties much superior to organic MBD (OMBD).[35] Highly ordered Pentacene films have been deposited,[36,37] characterized, and used to fabricate state-of-the-art field effect organic transistors,[9] showing features observed only in single crystals. The grain size in the films can be controlled by tuning the KE of the organic precursor in the supersonic beam, up to the point of inducing a layer by layer growth, so that the role of the grain boundaries is minimized and the film conductivity enhanced.[38] Similar results have been obtained for other molecules such as titanylphthalocyanine and oligothiophenes.[39,40]

Here we explore the extension of these concepts to the synthesis and growth of thin films of an hybrid host-guest Er-Tetraphenylporphyrin (Er-TPP) complex in an ultrahigh-vacuum (UHV) co-deposition experiment. To this end, we use pure erbium by MBE as guest partner and pure Tetraphenylporphyrin (H_2TPP) by SuMBD as the host. We then show that hybrid synthesis is achieved at the surface of the growing film, taking full advantage in this co-deposition scheme of the unique SuMBD growth conditions, in terms of precursor kinetics and purity. Our approach and results pave the way to the controlled preparation and exploration of classes of hybrid materials at the solid state that can be hardly obtained by wet chemistry. We therefore envision that such studies could highly contribute to the definition of classes of devices where the simultaneous control of chemistry, purity, interfaces, electronic, and structure at the different length scales is crucial, as it is often the case.

II. EXPERIMENTALS

The study has been performed at the IFN-CNR laboratory where an experimental setup, fully devoted to UHV thin-film growth and *in situ* analysis, has been developed. It is composed of two main UHV chambers connected by a UHV sample transfer system so that film deposition (but also simple electronic devices fabrication) and complete *in situ* electronic characterization can be performed without exposure to air contaminants. The first chamber is equipped with up to three supersonic beam and MBE evaporation sources. Thin-film growth can be achieved in a co-deposition scheme, with different material sources operating at the same time and combining both SuMBD and MBE approaches. The second chamber is equipped with several electron surface spectroscopies to perform films and interfaces physical, chemical and structural studies.

A supersonic beam source was used for the H_2TPP deposition.[31,32] It essentially consists of a quartz tube, with a nozzle (90 μm diameter) positioned at the front closed end, inside which a high-pressure carrier gas in injected. The powders of the organic are placed inside the source. The sublimation point can be easily achieved by means of an external heater, stabilized by an electronic feedback with a thermocouple. The SuMBD source operates in high vacuum: the gas mixture of gas carrier seeded by the organic vapors experience a supersonic expansion and, after skimming by a properly shaped conical collimator (skimmer), forms an highly collimated continuous molecular beam. The growth rates on the substrate can be easily varied from 0.1 Å/min up to 10 Å/min: a typical value of about 2 Å/min was used in our experiments. The H_2TPP material was supplied by Sigma Aldrich, with a nominal purity of 99.9%. Great care was devoted to fully purify and obtain a contaminant-free H_2TPP molecular beam in the SuMBD source, as verified by time of flight (TOF) mass spectrometry analysis. The carrier gas was He, with a typical working pressure inside the source of 1200 mbar at a temperature of about 240 °C. Under those operating conditions, the kinetic energy for the H_2TPP molecule was about 15 eV, while the speed ratio of the beam was typically $\geq$15, as evaluated by TOF.

Erbium was obtained from a TriCon electron-beam evaporator,[41] by means of which the material is efficiently evaporated in a Knudsen regime. A molecular beam of pure metallic erbium was produced after prolonged material outgassing, in order to avoid any presence of the metal oxide. We checked the purity of an erbium thin film by Auger-electron spectroscopy (AES) and x-ray photoelectron spectroscopy (XPS). The metal arrival rate on the substrate could be varied from 0.01 up to 10 Å/min: the value used in the present experiment was 0.24 Å/min. In these conditions, by taking into account the theoretical solid-state density of H_2TPP, we have evaluated that the ratio between the number of metal atoms and organic molecules at the film surface was about 4 ± 1 atom/molecule.

The substrates were made out of a silicon wafer (*n* type, 0.01 Ω cm), showing its own native oxide layer. Cleaning procedures were performed prior the insertion in vacuum by immersion in ultrasonic baths of trichloroethylene/acetone/isopropanol, followed by Joule thermal treatments up to 300 °C *in situ* in UHV, in order to eliminate the presence of contaminants, as confirmed by Auger and x-ray electron spectroscopies. In order to avoid the interference of any chemical process between the highly reactive lanthanide and the underlying oxide surface during the organic/inorganic co-deposition experiment, a 50 nm thin H_2TPP film was deposited on the native silicon oxide/Si(100). Afterwards, the Er-TPP compound was synthesized by co-deposition on the previously deposited organic film which, in turn, acts as a buffer layer between the oxide and the Er-TPP layers. In the adopted co-deposition approach, the organic supersonic and the inorganic atomic beams were used simultaneously. The substrate was kept at room temperature, with the SuMBD beam perpendicular to its surface and the MBE beam tilted of about 45° with respect to the surface normal. During co-deposition, the pressure in the chamber was about 5×10^{-8} mbar (base pressure 1×10^{-10} mbar) due to the He gas load from the supersonic beam, which in point of fact did not lead to any contamination in the growing film. The typical thickness of the co-deposited layer was about 60 nm, grown at a rate of $\sim$2 Å/min.

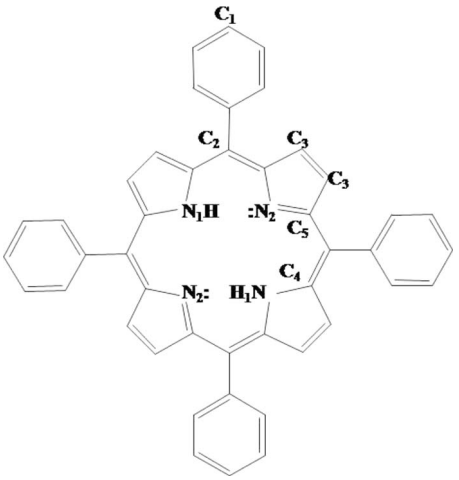

FIG. 1. Tetraphenylporphyrin H_2TPP molecule (planar representation). The different carbon and nitrogen atomic species are shown.

In the UHV analysis chamber we characterized the film surface using several techniques, such as AES, XPS, and ultraviolet photoelectron spectroscopy (UPS). XPS is performed using a nonmonochromatized Mg $K\alpha$ photon source (1253.6 eV), while the UV photons at 21.2 eV are obtained from a He discharge lamp. The electron energy analyzer, a VG CLAM2 hemispherical type, enables a total final-energy resolution of 0.95 eV for XPS and 0.15 eV for UPS, experimental conditions used for all the spectra shown in this work. The binding energies (BEs) have been calculated referring to a Au sputter cleaned surface, i.e., to the $4f$ 7/2 Au level at 84.0 eV for XPS and to the Fermi level for UPS.

The core-level analysis has been performed by Voigt line shape deconvolution after background subtraction by a Shirley function. The typical precision for peak energy positioning is $\pm$0.05 eV, uncertainty for full width at half maximum (FWHM) is less than 5% and for area evaluation is about 2.5%.

III. RESULTS AND DISCUSSIONS

Tetraphenylporphyrin ($C_{44}H_{30}N_4$) is composed of a macrocycle with four pyrrol rings (porphyrin), having four phenyl rings located in the meso positions, tilted with respect to the main molecule plane (Fig. 1, planar representation). Also taking into account the bond delocalization typical of π-conjugated aggregates, several atomic species can be identified in the molecule (see Fig. 1) by taking into account the different chemical environments experienced by each atom. Two types of nitrogen are present: the hydrogenated N_1 (two atoms) and the aza nitrogen atoms N_2 (two atoms), characterized by a free-electron lone pair (double dot in Fig. 1). Each phenyl is composed of six carbon atoms having the same chemical properties, named C_1 (24 atoms). The C_2 atoms in the meso position (four atoms) do not show any hydrogen bond. The two types of nonequivalent pyrrol rings

include: the C_3 type (eight atoms) having a bonding configuration quite similar to the C_1 species (but belonging to a pyrrol ring instead of a phenyl group), the C_4 type (six atoms), and the C_5 type (two atoms) characterized by having one single bond and one double bond with nitrogen, respectively. Since the delocalization of the C=N double bond in the pyrrol ring typically leads to a chemical equivalence of the two carbon atoms bonded to the aza nitrogen atoms, the number of C_4/C_5 could be 4/4 instead of 6/2.

In metal porphyrins, the guest species is usually located at the center of the macrocycle: the two hydrogen atoms are missing and the metal ion is coordinated with all the four nitrogen atoms. Typically, the oxidation number of the metal is +2, being in its doubly ionic state (e.g., for Zn, Fe, Mn). As far as Er is concerned, its ionic state is +3, but its coordination number can be as high as 9. This property is at the origin of the high reactivity of erbium. When Er-porphyrin complexes are prepared in solution, the metal is usually positioned at the center of the macrocycle while one or more other bonds are usually saturated by some other element or group.[42] Otsuki *et al.*[43] proposed the formation of complexes where one single Er is bonded to two different molecules, fully exploiting the high coordination number of the lanthanide.

From the analysis of the molecular orbitals (MOs) populations and distributions coming from UPS we get important indication on the chemical structure of the organic molecular film formed. Figure 2(a) compares the typical valence-band spectra for the pure H_2TPP and for the co-deposited Er-TPP film, while a blow up view of the highest occupied molecular orbital (HOMO) region is shown in Fig. 2(b). The two spectra show the presence of several structures forming similar patterns for the valence bands. In fact, the features in the 7–16 eV region of BEs are about the same in the two films, from both the quantitative and the qualitative points of view. On the other hand, the two peaks in the 0–6 eV range, located at about 2.5 eV (HOMO) and 4.5 eV, results to be modified and depleted in the Er-TPP film. Moreover, we observe the systematic presence of an underlying background in the co-deposited films that extends up to about 0.5 eV BE. A rigid shift toward higher BE of the whole Er-TPP spectrum was also observed. We believe that this trend is likely due to a change in the system work function or to the formation of dipole at the underlying interfaces, the latter being a typical effect of organic molecules deposited on metals and semiconductors.[44] To assess the origin of this shift, we have carefully evaluated the onset of the UPS spectrum. We observed the absence of effects due to dipole formation for H_2TPP/SiO_2, while for Er-TPP/H_2TPP we measured a systematic difference of $+0.4 \pm 0.1$ eV. This rigid shift, being due to a change in work function or to the formation of dipole at the interface, must be taken into account also for the XPS data described in the following. From the UPS spectra (by measuring the spectrum total length), we evaluated the (first) ionization potential of H_2TPP to be 6.2 eV, in good agreement with previously reported data.[22,45] A similar accurate and reliable estimate is difficult for Er-TPP due to the strong modification of the HOMO peak and of the underlying background.

Even though a detailed assignment of the spectral features to specific molecular orbitals is beyond the scope of this paper, it is worth discussing here some of the major structures observed. For the H_2TPP molecule, the peaks in the 7–16 eV range are typically related to π and σ orbitals generated by the phenyl carbon atoms C_1 and C_2 and to σ orbitals from nitrogens.[19,22,46] The HOMO structure at 2.5 eV BE is due to the a_{1u} and a_{2u} π orbitals, mainly delocalized on the pyrrol ring and involving both carbon and nitrogen atoms. These MOs are almost degenerate in H_2TPP while they are not in metal porphyrins. In fact, only a_{1u} is being responsible for the HOMO peak for several metal complexes, while the a_{2u} orbital is significantly stabilized and shifted to higher binding energies.[22,46] The band located at 4.5 eV is generally ascribed to π orbitals, again delocalized on the pyrrol ring but involving mainly C_3 and nitrogen atoms.

On the basis of this picture, a first indication arising from our UPS analysis is that the four phenyl groups and the meso bridges, C_1 and C_2 atoms, respectively, are not significantly involved in the interaction with Er. Conversely, only a sub-

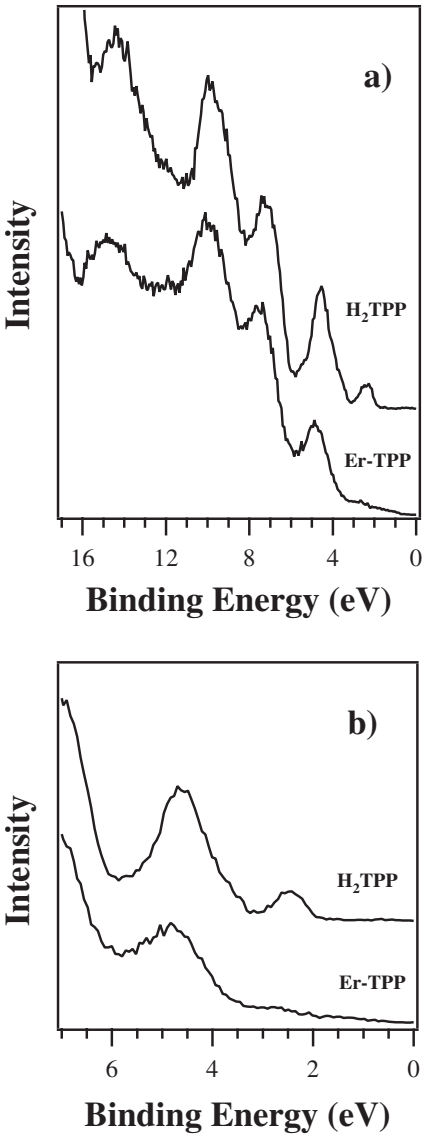

FIG. 2. (a) UPS (HeI 21.2 eV photon source) valence-band spectra from the H_2TPP film and from the Er-TPP film. (b) A detailed view of the HOMO region is also shown.

stantial charge rearrangement in the central macrocycle can both induce the strong reduction in the density of states observed in the HOMO and generate the important line shape modifications of the structure at 4.5 eV, in a way similar to what occurs in metal porphyrins and metal phthalocyanines.[22,46] In these molecules in fact, the contribution of metal states to the highest occupied MOs is usually very small with only minor peak shifts and no important line shape modifications of the HOMO with respect to a free base species. In our case, the other observed differences between the Er-TPP and H_2TPP spectra can be due to the peculiar electronic properties of Er.[14] In fact, similar MOs distributions have been found in the case of complexes with large metal atom (PbPc, Ref. 19) and in relativistic DFT calculations performed on Fe, Ru, and Os porphyrins.[47]

In our UPS spectra there is no clear evidence of signatures directly related to the Er electronic orbitals. As it is well known, emission related to the Er 4*f* state is located at about 6–10 eV for the atom in a metallic state and at higher BE for the oxidized form.[48,49] An evidence of the Er presence is the appearance of a significant background up to 0.5 eV, which is not present at all in the H_2TPP valence band where no signal can be detected at BEs lower than the HOMO peak. Once properly corrected for the mentioned shift of the Er-TPP UPS spectra ($+0.4 \pm 0.1$ eV), the background edge reduces from 0.5 eV to only $+0.1 \pm 0.1$ eV, a value that is very close to the Fermi edge of the Au reference used in our experiment. This is a strong indication of a decrease in the insulating character of the organic film, probably due to the formation of new states in the gap between HOMO and lowest unoccupied molecular orbital (LUMO) or to a better overlapping of the π MOs of the molecules in the film. The presence of a metallic network or clusters could also justify the presence of a quasi-Fermi edge. Even if the erbium atomic density in the molecular hybrid film should be about one order of magnitude lower than in the pure metal lattice, such a contribution cannot be fully excluded.

Further and more detailed information on the chemical properties of the hybrid material were achieved by the analysis of the core levels of the main atomic species present in the porphyrin molecules. Figure 3 shows the typical observed line shapes of the N 1*s* core level for both H_2TPP and Er-TPP films. In both cases the total area is the same, suggesting that no nitrogen losses have occurred during the co-deposition experiment.

The spectrum for the free base porphyrin is characterized by two main features, which well reflect the presence of two types of nitrogen atoms, as previously stated.[21,23,24] The Voigt line shape deconvolution (see Table I for details) leads to two main peaks, N_A and N_B, having the same FWHM of 1.05 eV and located at 401.60 and 399.60 eV, respectively. They are generated by the two different atomic species present in the molecule, the hydrogenated N_1-type atoms (N_A) and the aza N_2 type atoms (N_B), respectively. A third broad component N_S at 403.80 eV can also be identified: it is considered a shake up peak of the photoelectrons originating from the N_A feature and inducing a π-π^* resonant electron promotion process, coherently with previous observations.[21,23] It is expected that also the N_B peak should have a similar satellite that has not been considered here in the deconvolution. Such contribution would in effect partially sum on the N_A feature and could explain the slightly different weight of the two main peaks, 50.1% for N_A and 43.3% for N_B on the total N 1*s* signal, that should otherwise have the same area.

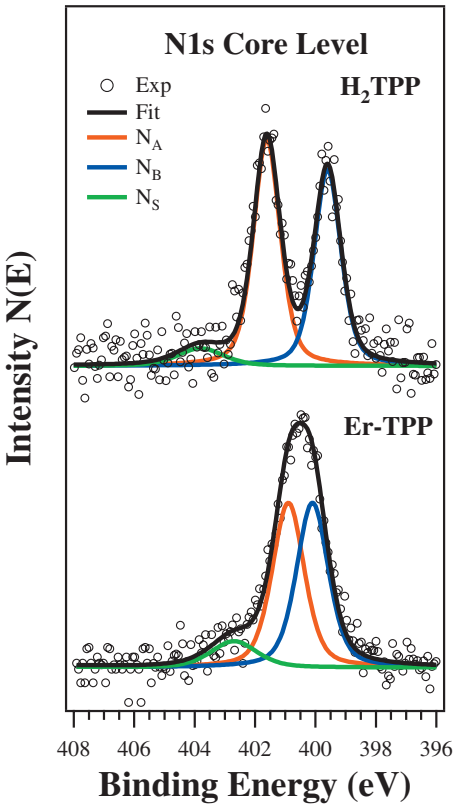

FIG. 3. (Color) N 1*s* core levels (background subtracted) from the H_2TPP film and from the Er-TPP film (empty circles). The peak deconvoluted components N_A, N_B, and N_S are shown (see text for details). The fit curve is the sum of the several components.

The N 1*s* peak line shape of the Er-TPP co-deposited films is completely different (Fig. 3), showing only one large feature with a broad satellite on the high BE side. The curve can be well reproduced by using a scheme similar to the one used for H_2TPP (see Table I for details): two peaks, N_A and N_B, having the same reciprocal weight (44.8% on total N 1*s* signal) and FWHM (1.25 eV) but located at 400.90 and 400.10 eV. The N_S satellite peak is now located at 402.70 eV

TABLE I. N 1*s* core-level deconvolution: components characteristics for the H_2TPP and Er-TPP films.

	Component	Binding energy (eV)	FWHM (eV)	Area% on N 1*s*
H_2TPP	N_A	401.60	1.05	50.1
	N_B	399.60	1.05	43.3
	N_S	403.80	1.80	6.6
Er-TPP	N_A	400.90	1.25	44.8
	N_B	400.10	1.25	44.8
	N_S	402.70	1.80	10.4

and is more pronounced than for the free base porphyrin, being about 10.4% of the total area instead of 6.6%. Its position is +1.80 eV from the N_A peak, that is, closer than for the free base molecule (+2.20 eV).

The N 1*s* core-level data give hence a clear evidence that the chemical properties of nitrogen atoms have been deeply modified in the molecules of the co-deposited hybrid film. In fact, the reduction in the energy gap between the N_A and N_B peaks is dramatic, from 2.0 down to 0.8 eV. The energy shifts for the two N_A and N_B components, with respect to the pristine H_2TPP molecule, are −0.7 and +0.50 eV, which become −1.10 and +0.10 eV, respectively, when corrected by the $+0.4 \pm 0.1$ eV shift observed in UPS. The FWHM of N_A and N_B peaks is higher than for H_2TPP, about +20%, while no significant change is observed on the width of the N_S satellite.

This reveals an important charge redistribution on the four nitrogen atoms that makes them much more chemically similar and equivalent than in the H_2TPP. The picture emerging and discussed in more details in the following is consistent and actually strengthens the analysis based on the UPS data, pointing to the formation of a metal-porphyrin complex. The final product, Er-TPP, is hence the synthesis of having one metal atom in the center of the macrocycle coordinated with the four nitrogen atoms. Indeed, our data are compatible with a reaction mechanism including the formation of covalent bonds between the metal and the N_1 atoms and the simultaneous loss of the two hydrogen atoms, while the aza N_2 becomes coordinated with the metal. In the resulting molecule, the four nitrogen atoms are chemically equivalent, as it is typical of the so-called "bridged" configuration reported by several authors.[21,23,24] Moreover, the charge rearrangement produces the excess in electron density observed on the macrocycle with respect to the central metal atom, which assumes the positive charge typical of a ionic state. This is confirmed by a shift of its core level toward higher binding energies, similar to the corresponding situation in metal oxides.[19,50] The N_1 type atoms typically show a reduction in electronegativity with respect to the bonding with hydrogen, as supported by a decrease in the binding energy of the associated N_A component. On the other hand, the N_2-type nitrogen atoms, characterized by lone pair σ orbitals localized on each nitrogen atom, get stabilized with respect to the native porphyrin molecule due to the overlapping with the metal orbitals,[46] leading to a weak increase in the N_B component binding energy.

Thus, SuMBD co-deposition produces porphyrin macrocycle modified with the metal atom being inserted in the molecule. In fact, N_1 atoms show chemical properties that could be explained considering the Er inclusion with the hydrogen bonds being lost. Indeed, a simple charge rearrangement could not account for the observed large energy shift. On the other hand, the N_2-type atoms appear to be less affected by the reaction, suggesting a weaker chemical interaction with a new chemical species as observed for host-guest molecular systems. The presence of a more intense satellite N_S (with respect to the free base molecule) is likely due to the superposition of the specific contributions of the two N_A and N_B components that are closer than in H_2TPP. However, a contribution could also come from the rearrangement of the LUMO density of state enhancing the shake up process.

The present data give only indirect information regarding the question if the mechanism giving rise to the Er inclusion in the H_2TPP molecule induces also the lost of the two hydrogen atoms. Indeed, unlike observations on other metal-TPP, the four nitrogen atoms are not fully equivalent since two different components can still be discriminated in the N 1*s* core-level emission. This feature cannot be ascribed to the simultaneous presence in our films of reacted and unreacted H_2TPP molecules, giving rise to a signal that is the superposition of both species. In fact, we have performed a detailed study as a function of the lanthanide concentration in the co-deposition experiment showing that the line shape remains the same even at erbium concentrations much larger than four Er atoms per H_2TPP molecule. A double N 1*s* peak structure from metal porphyrins has already been reported for strongly interacting systems such as Zn-TPP/C_{70} and attributed to the π^* MOs overlapping of the two molecules.[51] On the other hand, studies on polymers based on Zn-porphyrins have proved that the intermolecular interaction can alter the metal-atom coordination in the porphyrin and thus give rise to a double N 1*s* peak.[52] These are examples suggesting the presence of a strong chemical interaction involving the metal atom in the macrocycle that induces a significant nonequivalence of the four nitrogen atoms. Indeed, erbium is an atomic species that shows chemical properties, due to its complex electronic shells configuration, that could justify the observed differences with respect to the other studied metal porphyrins.[14] The presence of an intermediate chemical state, where Er is coordinated with the porphyrin but the N-H bonds are still present, as already reported[14] for other systems (Zn and H_2TPP), could be probably excluded. In fact, the energy difference between the two N 1*s* peaks for metalation experiments in Ref. 29 is about 1.7 eV, strictly and coherently similar to the 2.0 eV of the unperturbed molecule, but it is far from the 0.8 eV value measured in our experiments, more coherently similar to the 0.3 eV reported for Zn-porphyrin in strongly interacting systems. Moreover, it must be taken into account that erbium mass (167.26 amu) and atomic radius (175 p.m.) are much higher with respect to e.g., zinc (65.41 amu and 135 p.m., respectively). This is a factor that plays a role since the chemical interaction between the central metal atom and the organic molecule, in terms of molecular-orbital overlapping, strongly increases in presence of a smaller size of the coordinating cavity of the molecule.[46] An increase in the ratio between the dimensions of the guest metal atom and host macrocycle could in fact enhance the chemical interaction between the organic and the inorganic counterparts, giving rise to different and more complex chemical interactions in the Er-TPP with respect to other metal porphyrins. Finally, another prospect that cannot be presently ruled out is the formation of a more complex molecular aggregate, for example, a double-decker structure where the Er atom coordinates eight nitrogen atoms, belonging to two different porphyrin molecules.[43] The existence of such structures cannot be excluded or confirmed on the basis of the present experiments only; it requires further studies to be assessed.

Our experiments indicate that the chemical state of the metal atom resembles that of an oxidized state, as it occurs

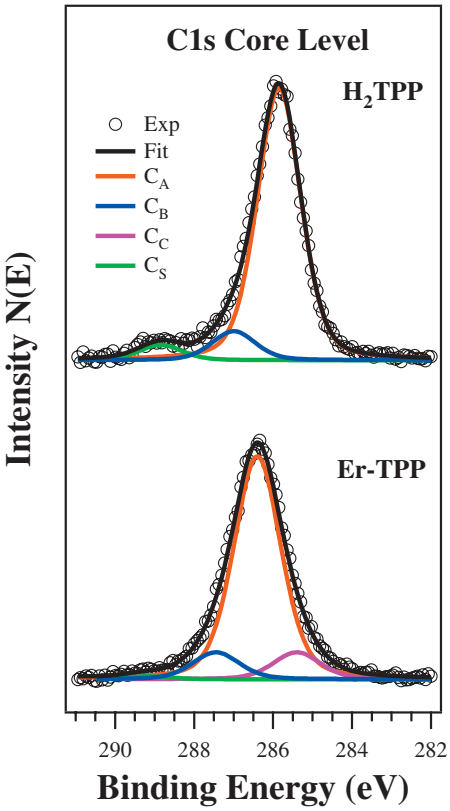

FIG. 4. (Color) C 1*s* core levels (background subtracted) from the H_2TPP film and from the Er-TPP film (empty circles). The peak deconvoluted components C_A, C_B, C_C, and C_S are shown (see text for details). The fit curve is the sum of the several components.

for other metal porphyrin.[24,50] In fact we have found that the Er 4*d* level is located at 170.3 eV (169.9 eV, taking into account the +0.4 eV shift of the entire spectra) and characterized by a single broad peak, in good agreement with the previously reported values of 170.4 eV for Er_2O_3 and significantly different from the metallic state,[53] located at about 167 eV and characterized by a double peak line shape.

Figure 4 shows the typical C 1*s* spectra for films of H_2TPP and Er-TPP, respectively. Both of them are clearly dominated by one main component, with the presence of less intense features. The two spectra do not show the large differences observed for the nitrogen emission, as observed in previous studies comparing the C 1*s* emission from free base and metal porphyrins.[21–27] However, some important consideration can be made. First of all, the total area is the same for the two peaks, i.e., no carbon atom losses have occurred during the co-deposition experiment. Moreover, the indication emerges that the molecule has not lost its original composition, which is consistent with the nitrogen data.

A more detailed analysis (see Table II) shows for H_2TPP the presence of a main component, C_A, at 285.85 eV (FWHM 1.30 eV) and of a second component, C_B, at 286.95 (FWHM 1.25 eV). A third feature, C_S, located at 288.85 eV (FWHM 1.30 eV) is also present, the origin of which is the same previously discussed for the N_S satellite (shake up peak of the photoelectrons originating from the C_A feature and inducing a π-π^* resonant electron promotion process). The

TABLE II. C 1*s* core-level deconvolution: components characteristics for the H_2TPP and Er-TPP films.

	Component	Binding energy (eV)	FWHM (eV)	Area% on C 1*s*
H_2TPP	C_A	285.85	1.30	86.0
	C_B	286.95	1.25	9.1
	C_S	288.85	1.30	4.9
Er-TPP	C_A	286.40	1.40	80.0
	C_B	287.40	1.40	9.5
	C_C	285.35	1.40	9.5
	C_S	289.20	1.40	1.0

percentages on the total C 1*s* area of the C_A and C_B peaks are, respectively, 86.0% and 9.1%, corresponding to emission from about 38 and 4 carbon atoms, becoming about 40 and 4 if corrected with the weight of the C_S peak. The identification of the different types of carbon atoms giving rise to the two major components C_A and C_B is not straightforward. On the basis of the relative chemical environment, the core levels of C_1- and C_3-type atoms should have characteristics quite similar to those of the C_2-type atoms in the meso positions.[21,27] The C_4-type atoms, single bonded with nitrogen and/or the C_5-type carbon atoms, double bonded with nitrogen, are expected to exhibit a markedly different BE, higher with respect to other carbon species due to the nature of the chemical bonds.[49] On this basis, the C_A component can be uniquely assigned to emission from C_1, C_2, C_3, and C_4 or C_5 while the C_B component from C_5 or C_4 atoms, respectively. This is in good agreement with the experimental value of carbon atoms originating from the two C_A and C_B peaks, respectively, about $40=36(C_1+C_2+C_3)+4(C_4$ or $C_5)$ and $4(C_5$ or $C_4)$. This compares well with other studies, when the total-energy resolution of our acquisition system is considered.[27]

Comparing the C 1*s* emission of Er-TPP with the free base porphyrin (Fig. 4), the C_A peak results to be shifted toward higher BE of +0.55 eV (reduced to $+0.15\pm0.1$ eV taking into account the observed rigid shift), while the C_B and C_A peaks become separated of +1.00 eV apart, instead of +1.10 eV (see Table II). All peaks show a FWHM of 1.40 eV, significantly higher than in the free base molecule. The C_S satellite becomes only 1% of the total, which is lower than for H_2TPP. We also observe a large broadening at the lower BE side of the C 1*s* emission peak that we could only fit by introducing a component, called C_C, located at −1.05 eV with respect to C_A. The C_A, C_B, C_C features represent about 80%, 9.5%, and 9.5% of the total C 1*s* emission, corresponding to emission from about 36, 4, and 4 carbon atoms, respectively.

The reduced intensity of the C_S peak suggests a different distribution of the LUMO states, as already observed for the corresponding satellite in the N 1*s* emission. Comparing to the H_2TPP molecule C 1*s* emission, the increased FWHM (about +10%) for all peaks, the shift of the C_B peak toward the C_A component, and the appearance of a feature (C_C) can all be explained by a rearrangement of the BE of the differ-

ent carbon chemical species due to the interaction with erbium.

In fact the presence of the metal atom, for both phthalocyanines and porphyrins,[21,22,54] is known to affect mainly only the electronic properties of the central macrocycle, with the external parts of the molecule, i.e., the four phenyls (C_1 type) as well as the carbon atoms in the meso position (C_2 type), that are practically unperturbed. This is also consistent with our analysis of the valence-band data (see Fig. 2) and N 1*s* core level, with an important charge redistribution involving only the four nitrogen atoms and, thus, all or part of the C_3, C_4, and C_5 carbon atoms in the pyrrol rings. In this framework, the 28 C_1 and C_2 atoms unambiguously contribute to the C_A component, a value lower than the 36 atoms experimentally found. The C_4 and C_5 atoms probably become more similar than in the free base molecule, with a reduced reciprocal BE distance as for the nitrogen atoms. Thus, the C_B component (C_4 or C_5 atoms) becomes closer to the C_A peak that has a contribution by emission from the four C_5 or C_4 atoms, respectively.

The interaction of the macrocycle with Er causes an excess of negative charge in the pyrrol rings, hence inducing a lowering of BE for the N 1*s* core level of the N_1 atoms (N_A component in Fig. 3) and, probably, to the four C_3 carbon atoms belonging to their pyrrol rings and giving origin to the C_C peak. The remaining (four) C_3 atoms will then give origin to a C 1*s* emission enveloped in the C_A component (as it is in the free base molecule), with a total number of 36 atoms contributing to this peak, in good agreement with our experimental data. The observed effects on the C 1*s* core level are hence all together consistent with a reactivity with the Er atom, which deeply modifies the chemical characteristics of the macrocycle, so that the overall picture coming out from our experiments is quite clear.

IV. CONCLUSIONS

We have demonstrated for the first time and studied in UHV the direct synthesis by co-deposition of an organolanthanide complex. This has been achieved by a supersonic beam seeded by a free base H_2TPP molecule and by a molecular effusive beam of metallic erbium in a co-deposition scheme. Differently from other metalation experiments,[28–30] where synthesis of the metal-porphyrin compounds have been achieved for a single monolayer film, the co-deposition approach used here led to the formation of a thin film showing a thickness suitable for applications in optoelectronic devices. The analysis of the MOs distribution by UPS has shown an important charge rearrangement in the Er-TPP molecule with respect to the free base species, located in the central macrocycle with the H_2TPP periphery that is not perturbed by the co-deposition experiment. The study of the N 1*s* and C 1*s* core levels reveals a significant higher chemical equivalence of the four nitrogen atoms with respect to the free base molecule, with the presence of an higher electron density on the four pyrrols. Thus, experimental data analysis point to the formation of an Er-TPP complex, where an erbium atom is inserted at the center of the porphyrin macrocycle. Differences observed with respect to typical electronic features of other metal-porphyrin can be probably related to the peculiar properties of the lanthanide species or to the formation of intermolecular aggregates. Concerning the lost of the two hydrogen atoms of the free base molecule, it seems likely that it indeed occurs in our experiment. However, we have only indirect evidences and further work is necessary to fully confirm this hypothesis.

Our result pave the way to a variety of chemical processes where the final products, possibly overcoming kinetically the potential barriers, are controlled by the initial parameters of the beams. On the basis of both the results discussed here and the already demonstrated ability of SuMBD of controlling molecular assembling,[9,32–40] we envisage the perspective of controlling simultaneously by this approach, the chemical pathways, morphology, and structure. Experiments in this directions are already being in progress.

ACKNOWLEDGMENTS

The authors are gratefully indebted to F. Siviero for stimulating discussions, C. Corradi, M Mazzola, and M. Pola for their valuable technical assistance. This work was financially supported by the Italian Ministry of University and Research, SYNERGY-MIUR-FIRB project under Grant No. RBN03S7XZ.

*Corresponding author. FAX: +39-0461-314875; iannotta@fbk.eu

[1] K. Kuriki, Y. Koike, and Y. Okamoto, Chem. Rev. **102**, 2347 (2002).
[2] J. Kido and Y. Okamoto, Chem. Rev. **102**, 2357 (2002).
[3] B. S. Harrison, T. J. Foley, M. Bouguettaya, J. M. Boncella, J. R. Reynolds, K. S. Schanzea, J. Shim, P. H. Holloway, G. Padmanaban, and S. Ramakrishnan, Appl. Phys. Lett. **79**, 3770 (2001).
[4] T. S. Kang, B. S. Harrison, T. J. Foley, A. S. Knefely, J. M. Boncella, J. R. Reynolds, and K. S. Schanzea, Adv. Mater. **15**, 1093 (2003).
[5] Z. X. Zhao, T. F. Xie, D. M. Li, D. J. Wang, and G. F. Liu, Synth. Met. **123**, 33 (2001).
[6] R. Pizzoferrato, L. Lagonigro, T. Ziller, A. Di Carlo, R. Paolesse, F. Mandoj, A. Ricci, and C. Lo Sterzo, Chem. Phys. **300**, 217 (2004).
[7] M. A. Baldo, M. E. Thompson, and S. R. Forrest, Nature (London) **403**, 750 (2000).
[8] H. Suzuki, J. Photochem. Photobiol., A **166**, 155 (2004).
[9] T. Toccoli, A. Pallaoro, N. Coppedè, S. Iannotta, F. De Angelis, L. Mariucci, and G. Fortunato, Appl. Phys. Lett. **88**, 132106 (2006).
[10] K. M. Kadish, K. M. Smith, and R. Guilard, *The Porphyrin Handbook* (Academic, New York, 2000).
[11] G. Simonneaux, P. Le Maux, Y. Ferrand, and J. Rault-Berthelot, Coord. Chem. Rev. **250**, 2212 (2006).

[12] J. C. G. Bünzli and C. Piguet, Chem. Soc. Rev. **34**, 1048 (2005).
[13] A. Polman and F. C. J. M. van Veggel, J. Opt. Soc. Am. B **21**, 871 (2004).
[14] P. C. Becker, N. A. Olsson, and J. R. Simpson, *Erbium Doped Fiber Amplifiers, Fundamentals and Technologies* (Academic, San Diego, 1999).
[15] J. B. Oh, K. L. Paik, J. W. Ka, S. G. Roh, M. K. Nah, and H. K. Kim, Mater. Sci. Eng., C **24**, 257 (2004).
[16] A. Clark, V. Terpugov, F. Medrano, M. Cervantes, and D. Soto, Opt. Mater. **13**, 355 (1999).
[17] S. Kera, Y. Yabuuchi, H. Yamane, H. Setoyama, K. K. Okudaira, A. Kahn, and N. Ueno, Phys. Rev. B **70**, 085304 (2004).
[18] A. Gerlach, F. Schreiber, S. Sellner, H. Dosch, I. A. Vartanyants, B. C. C. Cowie, T.-L. Lee, and J. Zegenhagen, Phys. Rev. B **71**, 205425 (2005).
[19] N. Papageorgiou, Y. Ferro, E. Salomon, A. Allouche, J. M. Layet, L. Giovanneli, and G. Le Lay, Phys. Rev. B **68**, 235105 (2003).
[20] L. Cao, H. Z. Chena, L. Zhua, X. B. Zhangb, and M. Wang, Mater. Lett. **57**, 4309 (2003).
[21] Y. Niwa, H. Kobayashi, and T. Tsuchiya, J. Chem. Phys. **60**, 799 (1974).
[22] L. Scudiero, D. E. Barlow, U. Mazur, and K. W. Hipps, J. Am. Chem. Soc. **123**, 4073 (2001).
[23] J. C. Goll, K. T. Moore, A. Ghosh, and M. J. Therien, J. Am. Chem. Soc. **118**, 8344 (1996).
[24] G. Polzonetti, A. Ferri, M. V. Russo, G. Iucci, S. Licoccia, and R. Paolesse, J. Vac. Sci. Technol. A **17**, 832 (1999).
[25] M. P. de Jong, R. Friedlein, S. L. Sorensen, G. Öhrwall, W. Osikowicz, C. Tengsted, S. K. M. Jönsson, M. Fahlman, and W. R. Salaneck, Phys. Rev. B **72**, 035448 (2005).
[26] G. Polzonetti, V. Carravetta, G. Iucci, A. Ferri, G. Paolucci, A. Goldoni, P. Parent, C. Laffon, and M. V. Russo, Chem. Phys. **296**, 87 (2004).
[27] C. Castellarin Cudia, P. Vilmercati, R. Larciprete, C. Cepek, G. Zampieri, L. Sangaletti, S. Pagliara, A. Verdini, A. Cossaro, L. Floreano, A. Morgante, L. Petaccia, S. Lizzit, C. Battocchio, G. Polzonetti, and A. Goldoni, Surf. Sci. **600**, 4013 (2006).
[28] J. M. Gottfried, K. Flechtner, A. Kretschmann, T. Lukasczyk, and H.-P. Steinrück, J. Am. Chem. Soc. **128**, 5644 (2006).
[29] T. E. Shubina, H. Marbach, K. Flechtner, A. Kretschmann, N. Jux, F. Buchner, H.-P. Steinrück, T. Clark, and J. M. Gottfried, J. Am. Chem. Soc. **129**, 9476 (2007).
[30] T. Lukasczyk, K. Flechtner, L. R. Merte, N. Jux, F. Maier, J. M. Gottfried, and H.-P. Steinrück, J. Phys. Chem. C **111**, 3090 (2007).
[31] G. Scoles, *Atomic and Molecular Beam Methods* (Oxford University Press, Oxford, 1988).
[32] S. Iannotta, in *Cluster Beam Synthesis on Nano-Structured Materials*, edited by P. Milani and S. Iannotta (Springer, Berlin, 1999).
[33] R. Verucchi, L. Aversa, G. Ciullo, A. Podestà, P. Milani, and S. Iannotta, Eur. Phys. J. B **26**, 509 (2002).
[34] L. Aversa, R. Verucchi, A. Boschetti, A. Podestà, P. Milani, and S. Iannotta, Mater. Sci. Eng., B **101**, 169 (2003).
[35] S. Iannotta and T. Toccoli, J. Polym. Sci. [B] **41**, 2501 (2003).
[36] L. Casalis, M. F. Danisman, B. Nickel, G. Bracco, T. Toccoli, S. Iannotta, and G. Scoles, Phys. Rev. Lett. **90**, 206101 (2003).
[37] R. Ruiz, D. Choudhary, B. Nickel, T. Toccoli, K. C. Chang, A. C. Mayer, P. Clancy, J. M. Blakely, R. L. Headrick, S. Iannotta, and G. G. Malliaras, Chem. Mater. **16**, 4497 (2004).
[38] Y. Wu, T. Toccoli, N. Koch, E. Iacob, A. Pallaoro, P. Rudolf, and S. Iannotta, Phys. Rev. Lett. **98**, 076601 (2007).
[39] K. Walzer, T. Fritz, K. Leo, T. Toccoli, A. Pallaoro, R. Verucchi, A. Boschetti, and S. Iannotta, Surf. Sci. **573**, 346 (2004).
[40] T. Toccoli, A. Boschetti, P. Scardi, G. Barbarella, G. Sotgiu, and S. Iannotta, Philos. Mag. B **82**, 485 (2002).
[41] R. Verucchi and S. Nannarone, Rev. Sci. Instrum. **71**, 3444 (2000).
[42] P. D. Harvey, C. Stern, C. P. Gros, and R. Guilard, Coord. Chem. Rev. **251**, 401 (2007).
[43] J. Otsuki, S. Kawaguchi, T. Yamakawa, M. Asakawa, and K. Miyake, Langmuir **22**, 5708 (2006).
[44] A. Kahn, N. Koch, and W. Gao, J. Polym. Sci., Part B: Polym. Phys. **41**, 2529 (2003).
[45] D. P. Piet, D. Danovich, H. Zuilhof, and E. J. R. Sudhölter, J. Chem. Soc., Perkin Trans. 2 **1999**, 1653.
[46] E. J. Baerends, G. Ricciardi, A. Rosa, and S. J. A. van Gisbergen, Coord. Chem. Rev. **230**, 5 (2002).
[47] M.-S. Liao and S. Scheiner, Chem. Phys. **285**, 195 (2002).
[48] N. Guerfi, O. Bourbia, and S. Achour, Mater. Sci. Forum **480-481**, 193 (2005).
[49] S. Hüfner, *Photoelectron Spectroscopy* (Springer, Berlin, 2003).
[50] L. Scudiero, D. E. Barlow, and K. W. Hipps, J. Phys. Chem. **104**, 11899 (2000).
[51] P. Vilmercati, C. Castellarin Cudia, R. Larciprete, C. Cepek, G. Zampieri, L. Sangaletti, S. Pagliara, A. Verdini, A. Cossaro, L. Floreano, A. Morgante, L. Petaccia, S. Lizzit, C. Battocchio, G. Polzonetti, and A. Goldoni, Surf. Sci. **600**, 4018 (2006).
[52] D. M. Sarno, L. J. Matienzo, and W. E. Jones, Jr., Inorg. Chem. **40**, 6308 (2001).
[53] S. Kennou, S. Ladas, M. G. Grimaldi, T. A. Nguyen Tan, and J. Y. Veuillen, Appl. Surf. Sci. **102**, 142 (1996).
[54] T. Yamada, T. Manaka, H. Hoshi, K. Ishikawa, and H. Talezoe, J. Porphyr. Phthalocyanines **2**, 133 (1998).